A phenomenological model of the fundamental power coupler for a superconducting resonator

Ran Huang[1,*], Yuan He [1,*]

[1] Institute of Modern Physics, Chinese Academy of Sciences, Lanzhou 730000, China

*Corresponding author, burn4028@impcas.ac.cn and hey@impcas.ac.cn

This work was supported by the CAS "Light of West China" Program (No. 29Y936020), National Natural Science Foundation of China (No. 12105331), and Strategic Priority Research Program of the Chinese Academy of Sciences (No. XDB34010102).

Abstract

In this study, a phenomenological model of the radio frequency (RF) behavior of a superconducting cavity fundamental power coupler is proposed by analyzing the simulation results of a transient beam loading process in an extremely over-coupled superconducting cavity. Using this phenomenological model, the calculation of the transient reflected power from a superconducting cavity under beam loading can be mathematically simplified to algebraic operations without solving the differential equation governing the transient beam loading process, while maintaining the calculation accuracy. Moreover, this phenomenological model can facilitate an intuitive understanding of the significant surge in the time evolution of reflected power from a superconducting cavity in certain beam-loading processes. The validity of this phenomenological model was carefully examined in various beam loading processes and cavity conditions, and the method based on this phenomenological model was utilized in the transient RF analysis of the superconducting cavity system of the CAFe Linac, achieving satisfactory results.

Keywords: Power Coupler, Reflected Power, Superconducting Cavity, Beam Loading

1 Introduction

The calculation of the transient power reflected from a high-Q-value resonator under extreme over-coupling has practical significance in the field of microwave engineering because the excessive reflected power from this resonator under certain conditions may damage the radio frequency (RF) system. A superconducting RF cavity [1-3] , adopted to accelerate the charged particle beams in an accelerator [4-6], is a typical high-Q-value resonator with intrinsic Q-values typically $\geq 10^8$ and loaded Q-values [7] usually $\geq 10^5$ due to the extremely low RF-power loss in the cavity wall owing to the superconductivity of niobium [8, 9] at ultra-low temperatures [10]. Unlike a normal conducting cavity with a loaded Q-value, typically in the order of 10^3 and near critical coupling, the transient power reflected from a superconducting cavity in certain beam-loading processes can attain values several times larger than the RF generator forward power [11] , thus has a high potential to damage the RF power system, particularly the circulator, which is usually designed to withstand as large as the forward generator power considering a full reflection situation. Therefore, it is critical to calculate the time evolution of the reflected power from a superconducting cavity during various transient beam loading processes to provide the necessary information for the design of an RF power system and a machine protection system [12], the latter one can prevent the RF power system of an accelerator from being accidentally damaged and increase its availability. In existing calculation

methods [13, 14], the transient power reflected from a superconducting cavity under beam loading can only be obtained by analytically or numerically solving the differential equation governing the transient beam-loading process inside the cavity, which is relatively complicated and can be time-consuming. For certain specific requirements, such as designing a high-level RF system concerning the RF power waveguide or the circulator between an RF power generator and a superconducting cavity, the transient power reflected from the superconducting cavity in various processes is the RF quantity of interest, instead of the time evolution of the RF fields inside the cavity [15-17], the analysis for the latter one is usually performed by low-level RF system engineering [18-20]. Therefore, a method to directly calculate the reflected power without numerically solving the beam-loading differential equations was researched. In this study, we reported a method based on a novel phenomenological model of a fundamental power coupler to fulfill the aforementioned goal, which has been facilitating the transient RF analysis of the superconducting cavity system of the CAFe Linac [21-23]. Thus, a phenomenological model of RF behavior of the fundamental power coupler [24] for a superconducting cavity under heavy beam loading was obtained by investigating the simulation results of a superconducting cavity in a transient beam-loading process without directly analyzing the corresponding differential equations governing such a process. Heavy beam loading refers to the case where the beam power is several orders of magnitude larger than the RF power loss in the superconducting cavity wall. Using this phenomenological model, the transient power reflected from a superconducting cavity can be converted into algebraic operations without solving the related differential equations. To verify its validity, the transient reflected power in several beam-loading processes was evaluated using the proposed model, and the results are compared with those obtained with the numerical method needing to solve the related differential equations. Moreover, the phenomenological model can analytically deduce the maximum transient reflected power during a superconducting cavity failure recovery process in an extremely high-availability accelerator, such as the one used for the accelerator-driven sub-critical system (ADS) application.

2 Existing calculation method and result analysis

2.1 Mathematical model on transient beam loading

In the conventional calculation method, it is necessary to solve the following equations governing the transient beam-loading process analytically or numerically to obtain the transient power reflected $P_{\mathrm{r}}(t)$ from a superconducting cavity under the Gaussian bunched beam loading [25]:

$$\frac{\mathrm{d}}{\mathrm{d}t}\vec{V}_{\mathrm{c}}(t)+\left(\omega_{0.5}+\mathbf{i}\Delta\omega\right)\vec{V}_{\mathrm{c}}(t)=\frac{\omega_{0.5}r_{\mathrm{c}}}{2(1+\beta)}\left(4\sqrt{\frac{\beta P_{\mathrm{g}}(t)}{r_{\mathrm{c}}}}e^{\mathrm{i}\theta(t)}-2I_{\mathrm{b0}}(t)T_{\mathrm{tf}}\,\mathrm{e}^{-\frac{\phi_{0.5}^2}{2}}\right), \tag{1}$$

and

$$P_{\mathrm{r}}(t)=P_{\mathrm{g}}(t)-\frac{V_{\mathrm{c}}^{2}(t)}{r_{\mathrm{c}}}-I_{\mathrm{b0}}(t)T_{\mathrm{tf}}\,\mathrm{e}^{-\frac{\phi_{0.5}^2}{2}}V_{\mathrm{c}}(t)\cos\left[\phi(t)\right]-\frac{2V_{\mathrm{c}}(t)}{\omega\left(\frac{r}{Q}\right)}\frac{\mathrm{d}V_{\mathrm{c}}(t)}{\mathrm{d}t}\ , \tag{2}$$

where $\mathbf{i}$ is the imaginary unit, $\vec{V}_{\mathrm{c}}(t)=V_{\mathrm{c}}(t)\exp\left[\mathbf{i}\cdot\phi(t)\right]$ is the phasor of the cavity voltage without the transit time factor T_{tf}; ω, $\omega_{0.5}$, and $\Delta\omega=\omega-\omega_0$ are the angular frequency, loaded half bandwidth, and detuning of the cavity, respectively. r_{c} and r/Q are the intrinsic shunt

impedance and r over Q of the cavity without T_{tf}, respectively; β is the coupling factor, $P_g(t)$ is the forward generator power, $\theta(t)$ is the phase of the effective driven current from the generator, $I_{b0}(t)$ is the time-averaged DC beam current, and $\phi_{0.5}=\omega\sigma_t$ is the half phase width of the Gaussian bunch (the effect of the beam current intensity on the bunch length is neglected here).

It can be mathematically proven that $\vec{V}_c(t)$ can be analytically solved using the Laplace transformation method when the time evolutions of $P_g(t)$ and $I_{b0}(t)$ in Eq. (1) conform to Eqs. (3) and (4) respectively, which is sufficient to describe a typical beam-loading process in a superconducting cavity [25]:

$$P_g(t)=\begin{cases} P_{g,1} & 0\le t<t_1 \\ P_{g,1}+\left[\dfrac{3(t-t_1)^2}{\Delta t_1^{\,2}}-\dfrac{2(t-t_1)^3}{\Delta t_1^{\,3}}\right](P_{g,2}-P_{g,1}) & t_1\le t<t_1+\Delta t_1 \\ P_{g,2} & t_1+\Delta t_1\le t<t_2 \\ P_{g,2}+\left[\dfrac{3(t-t_2)^2}{\Delta t_2^{\,2}}-\dfrac{2(t-t_2)^3}{\Delta t_2^{\,3}}\right](P_{g,3}-P_{g,2}) & t_2\le t<t_2+\Delta t_2 \\ P_{g,3} & t\ge t_2+\Delta T \end{cases}, \tag{3}$$

$$\text{and}\quad I_{b0}(t)=\begin{cases} I_{b1} & 0\le t<t_{b,1} \\ I_{b2} & t_{b,1}\le t<t_{b,2} \\ I_{b3} & t_{b,2}\le t<t_{b,3} \end{cases}. \tag{4}$$

Substituting the resultant $\vec{V}_c(t)$ into Eq. (2), $P_r(t)$ can therefore be analytically obtained .

2.2 Simulation result and analysis

The designed RF parameters of the HWR010 [26] and RF power generator of CAFe Linac, along with the designed beam parameters, are listed in Table 1, the transient beam loading process can be simulated using these parameters and Eqs. (1)–(4).

Table 1. RF and Beam Parameters for the evaluation

Parameters	Value
Mode frequency, f_0 (MHz)	162.5
r over Q (Ω)	147.84
Intrinsic quality factor, Q_0	8×10^8
Optimum coupling, β_{opt}	800
Transit time factor, T_{tf}	0.8
Forward generator power, P_g (kW)	6.7
Phase of the generator current, θ	-π/6
Synchronous phase, ϕ	-π/6
Half phase width of the bunch, $\Delta\phi_{0.5}$	π/12
Design beam current, I_b (mA)	10

Generator power rising edge, Δt_i (μs)	10
Generator power falling edge, Δt_i (μs)	10

The time evolution of the generator power and beam current in this process are shown in Fig. 1 (a). At $t_0 = 0$, the generator is powered up at 6.7 kW, and the cavity field buildup process begins. At $t_1 = \Delta T$, the continuous-wave (CW) proton beam began injecting at the designed current of 10 mA as the cavity field reached a certain steady state I with an amplitude of 1.72 MV and phase of zero. Owing to the beam loading effects, the field in the cavity evolved to steady state II with an amplitude of 1.00 MV and phase of –29.8°. At $t_2 = 2\Delta T$, the generator power was suddenly shut down and the beam continued passing through the cavity at 10 mA current, which is typical for a Linac used for ADS application to avoid a thermal shock to the reactor core due to the beam trip. This resulted in steady state III with a cavity field amplitude of 0.987 MV and phase of -150°. At $t_3 = 3\Delta T$, the generator power was recovered to 6.7 kW, and the field in the cavity restored to steady state II. During the entire process, the detuning angle of the cavity Ψ maintained its optimum value for stage II with the designed beam current intensity, which is as follows:

$$\psi_{\text{opt}} \approx -\phi \approx \pi/6 . \tag{5}$$

In the simulation, we used $\Delta T \approx 8\tau$ to ensure that the cavity fields can reach the corresponding steady state at each stage. Fig. 1 (b)–(f) presents the time evolution of the trace of the cavity voltage on the complex plane, cavity voltage amplitude, phase, reflected power, and kinetic energy gain of the central particle in a beam bunch, respectively. The simulation results shown in Fig. 1 were analyzed to obtain a phenomenological model of the fundamental power coupler for a superconducting cavity.

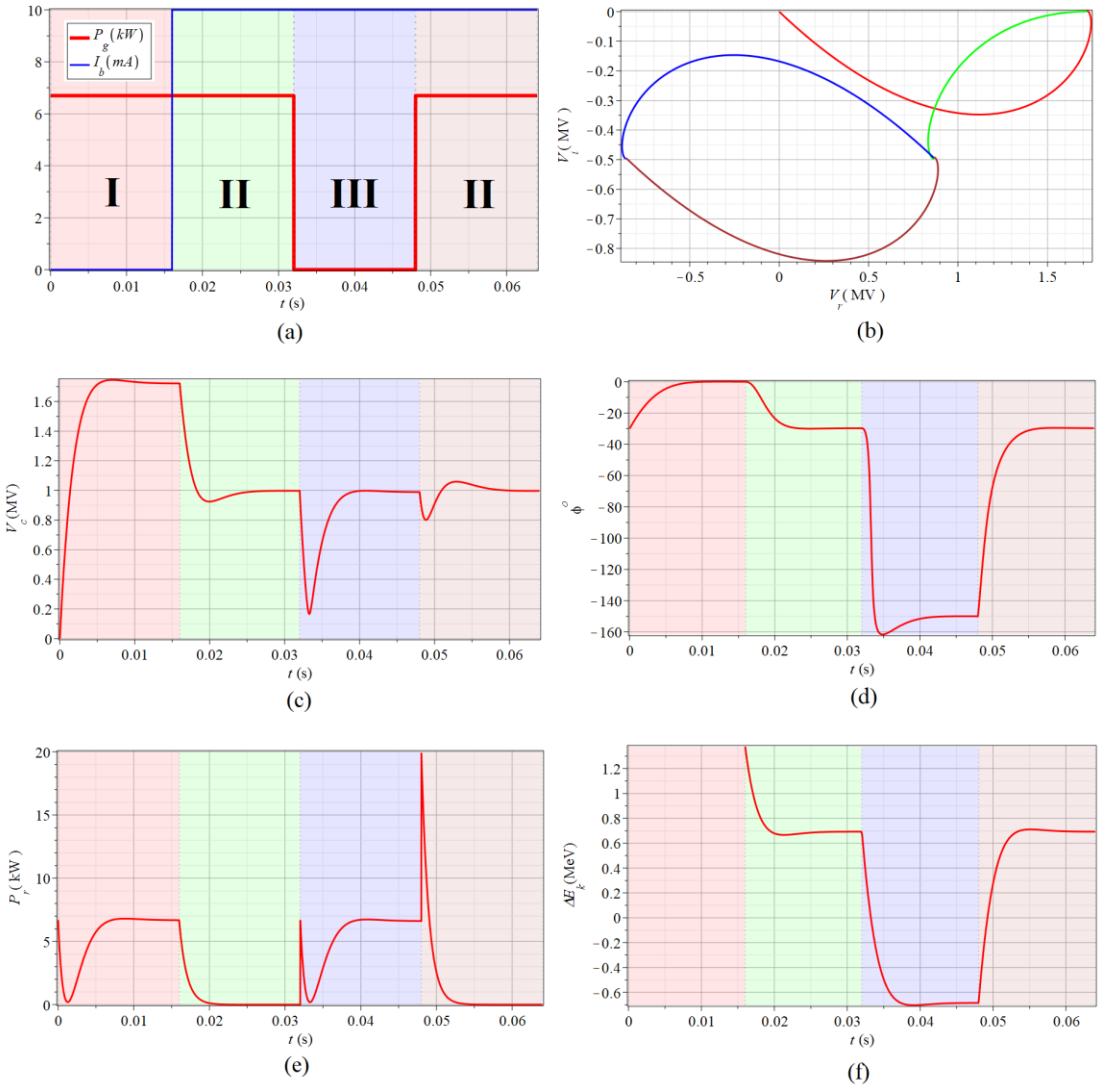

Fig. 1 (Color online) A superconducting cavity transient beam-loading process

(a) Generator Power and Beam Current (b) Trace of the Cavity Voltage (c) Amplitude of the Cavity Voltage

(d) Phase of the Cavity Voltage (e) Reflected Power of the Cavity (f) Energy Gain of the Central Particle

Fig. 1 (c) demonstrates that the amplitude of the cavity voltage in steady state III is the same as that at steady state II.

$$\left|\overrightarrow{V_{c,3}}\right| = \left|\overrightarrow{V_{c,2}}\right| \quad . \tag{6}$$

At steady state II, the cavity voltage $\overrightarrow{V_{c,2}}$ is the superposition of the generator-induced voltage $\overrightarrow{V_{g,2}}$ and the beam-induced voltage $\overrightarrow{V_{b,2}}$:

$$\overrightarrow{V_{c,2}} = \overrightarrow{V_{g,2}} + \overrightarrow{V_{b,2}} \, . \tag{7}$$

In steady-state III, owing to the absence of the generator power, the cavity voltage $\overrightarrow{V_{c,3}}$ is solely induced by the beam:

$$\overrightarrow{V_{c,3}} = \overrightarrow{V_{b,3}} \quad . \tag{8}$$

Using Eqs. (6) – (8), the following is obtained:

$$\left|\overrightarrow{V_{\mathrm{b},3}}\right|=\left|\overrightarrow{V_{\mathrm{g},2}}+\overrightarrow{V_{\mathrm{b},2}}\right| \quad . \tag{9}$$

Note, the beam current intensity remains constant during stages II and III, $\overrightarrow{V_{\mathrm{b},2}}=\overrightarrow{V_{\mathrm{b},3}}=\overrightarrow{V_{\mathrm{b}}}$, and Eq. (9) can be rewritten as follows:

$$\left|\overrightarrow{V_{\mathrm{b}}}\right|=\left|\overrightarrow{V_{\mathrm{g},2}}+\overrightarrow{V_{\mathrm{b}}}\right| \quad . \tag{10}$$

This indicates that the amplitude of the beam-inducing voltage is the same as that of the cavity voltage produced by the generator along with the beam, which is the case for a superconducting cavity under optimum coupling and detuning [13].

As shown in Fig. 1 (d), although the cavity voltage amplitudes at steady states II and III are identical, there is a difference of $2\pi/3$ in their phases, which results in the deceleration of the beam at steady state III, as shown in Fig. 1 (f). This can be explained through the conservation of energy principle, where the field in the cavity is induced solely by the beam in this state. In addition, Fig. 1 (e) indicates that the reflected powers at steady states II and III are significantly different. At steady state II, the optimum detuning and coupling of the cavity ensure zero-power reflection, whereas at steady state III, the cavity functions as a klystron, where the beam power is drawn out by the cavity and radiates to the waveguide through the coupler. Note, the transient reflected power is three times as large as the generator forward power at $t_3=3\Delta T$ when the generator power is recovered. The excessive reflection power is due to the change in the stored energy inside the cavity, which corresponds to the last term in Eq. (2).

3 Relationship between the voltage waves in the waveguide

3.1 Amplitude relationship between the voltage waves

According to the terminology of microwave engineering [27], the reflected power from the cavity $P_{\mathrm{r}}(t)$ in the previous sections is termed as “backward power in the waveguide” and is referred to as “backward power” for conciseness in the following sections. Meanwhile, to maintain brevity, the symbol a is used to denote the amplitude of a phasor $\vec{a}$, that is $a=\left|\vec{a}\right|$.

According to the theory of transmission lines, the traveling wave power in a waveguide can be expressed by the amplitude of the normalized equivalent voltage wave v as follows [28]:

$$P=v^2 \quad , \tag{11}$$

where $v=V/\sqrt{Z_0}$, V is the amplitude of the normalized equivalent voltage wave, and Z_0 is the characteristic impedance of the waveguide.

Based on Eq. (11), the following can be obtained:

$$v=\sqrt{P} \quad . \tag{12}$$

In the following analysis, the normalized equivalent voltage wave amplitude v that was determined using Eq.(12) is termed “voltage wave” for brevity.

The backward voltage wave (“backward wave”) $\overrightarrow{v_{\mathrm{bk}}}$ in the waveguide comprises the following two components:

1) Reflected voltage wave at the coupler ("reflected wave") $\vec{v}_r$, which is the direct reflection of the forward voltage wave ("forward wave") from the generator $\vec{v}_f$ at the coupler.

2) Radiated voltage wave from the cavity ("radiated wave") $\vec{v}_e$, which corresponds to the power radiated out of the cavity back into the waveguide through the coupler.

$$\vec{v}_{bk} = \vec{v}_r + \vec{v}_e \quad . \tag{13}$$

As shown in Fig. 1(e), when the cavity is under optimum coupling and optimum detuning, and the beam current is at the designed value, the backward wave at steady state II vanishes, i.e., $\vec{v}_{bk,2} = 0$; therefore, the following can be obtained:

$$\vec{v}_{e,2} = -\vec{v}_{r,2} \, . \tag{14}$$

This indicates that the reflected and radiated waves had the exact same amplitudes and opposite phases at steady state II.

The amplitude of the cavity voltage at steady state III is equal to that at steady state II, note that $v_e \propto V_c$; therefore the following can be obtained:

$$v_{e,3} = v_{e,2} \, . \tag{15}$$

For a cavity with beam loading, the cavity voltage $\vec{V}_c$ is the superposition of the generator-induced voltage $\vec{V}_g$ and the beam-induced voltage $\vec{V}_b$, i.e., $\vec{V}_c = \vec{V}_g + \vec{V}_b$. Similarly, the radiated wave $\vec{v}_e$ through the coupler can also be composed of two parts, including the contribution from the generator $\vec{v}_g$ and that from the beam $\vec{v}_b$:

$$\vec{v}_e = \vec{v}_g + \vec{v}_b \quad , \tag{16}$$

with the following relationships:

$$\begin{aligned} \vec{v}_g &\propto \vec{V}_g \\ \vec{v}_b &\propto \vec{V}_b \end{aligned} \quad . \tag{17}$$

At steady state III, the generator is powered down, and $\vec{v}_{f,3} = 0$. Note that $\vec{v}_{r,3} \propto \vec{v}_{f,3}$; therefore, $\vec{v}_{r,3} = 0$ and the resulting backward wave can be written as follows:

$$\vec{v}_{bk,3} = \vec{v}_{r,3} + \vec{v}_{e,3} = \vec{v}_{e,3} \quad . \tag{18}$$

Fig. 1 (e) demonstrates that the backward power at steady state III is equal to that at steady state I, indicating that the amplitudes of the corresponding backward waves should be identical:

$$v_{bk,3} = v_{bk,1} \, . \tag{19}$$

Note, there is no beam in the cavity at steady state I due to the extreme over-coupling of the cavity ($\beta \gg 1$), and the reflection coefficient of the cavity is $\vec{\Gamma} \to 1$; therefore, the following can be obtained:

$$\vec{v}_{bk,1} = \vec{\Gamma}\vec{v}_{f,1} = \vec{v}_{f,1} \quad . \tag{20}$$

The forward power from the generator remains constant at steady states I and II:

$$\overrightarrow{v_{\mathrm{f},2}} = \overrightarrow{v_{\mathrm{f},1}} \quad . \tag{21}$$

Using Eqs. (14)–(21), the following amplitude relationship can be deduced:

$$v_{\mathrm{bk},3} = v_{\mathrm{bk},1} = v_{\mathrm{e},3} = v_{\mathrm{e},2} = v_{\mathrm{r},2} = v_{\mathrm{b},2} = v_{\mathrm{f},2} = v_{\mathrm{f},1} \quad , \tag{22}$$

and thus

$$v_{\mathrm{r},2} = v_{\mathrm{f},2} \, . \tag{23}$$

This indicates that the amplitude of the wave directly reflected from the forward wave at the coupler is exactly equal to the amplitude of the forward wave at steady state II. In simple terms, the forward wave is fully reflected by the coupler.

The proportion of the forward wave reflected directly from the coupler is determined by the geometric structure of the coupler alone, which corresponds to the coupling factor β. Therefore, if β is fixed, the proportion of the forward wave directly reflected by a certain coupler should also be fixed. Note that β remains constant throughout the entire process; therefore, the following is obtained:

$$v_{\mathrm{r},i} \equiv v_{\mathrm{f},i} \qquad (i = 1..3) \, . \tag{24}$$

This indicates that the forward wave is fully reflected at the coupler during the entire process.

3.2 Phase relationship between the voltage waves

Let the phase of $\overrightarrow{v_{\mathrm{r},2}}$ be π, and using Eq. (23), $\overrightarrow{v_{\mathrm{r},2}}$ can be expressed as follows:

$$\overrightarrow{v_{\mathrm{r},2}} = -v_{\mathrm{f},2} \, . \tag{25}$$

Substituting it into Eq. (14) results in the following:

$$\overrightarrow{v_{\mathrm{e},2}} = v_{\mathrm{f},2} \, . \tag{26}$$

At steady state I, the cavity voltage $\overrightarrow{V_{\mathrm{c},1}}$ is induced by the generator alone. Considering the phase of the equivalent current of the beam as the reference phase, the phase of $\overrightarrow{V_{\mathrm{c},1}}$ is as follows:

$$\arg\left(\overrightarrow{V_{\mathrm{c},1}}\right) = \theta + \psi \quad , \tag{27}$$

where $\arg\left(\overrightarrow{V_{\mathrm{c},1}}\right)$ indicates obtaining the principal argument of $\overrightarrow{V_{\mathrm{c},1}}$.

The phase of the cavity voltage $\overrightarrow{V_{\mathrm{c},2}}$ at steady state II was the synchronous phase:

$$\arg\left(\overrightarrow{V_{\mathrm{c},2}}\right) = \phi \, . \tag{28}$$

For a coupler with a fixed geometric structure, the phase advance of the electromagnetic wave transmitted through the coupler must also be fixed; thus, the phase difference between $\overrightarrow{v_{\mathrm{e},2}}$ and $\overrightarrow{v_{\mathrm{e},1}}$ is equal to that between $\overrightarrow{V_{\mathrm{c},2}}$ and $\overrightarrow{V_{\mathrm{c},1}}$:

$$\arg\left(\overrightarrow{v_{e,2}}\right)-\arg\left(\overrightarrow{v_{e,1}}\right)=\arg\left(\overrightarrow{V_{c,2}}\right)-\arg\left(\overrightarrow{V_{c,1}}\right)=\phi-\theta-\psi \quad . \tag{29}$$

When the cavity is under optimum coupling and detuning, and the beam current is at the design value, the equivalent impedance of the beam-cavity system is real, indicating that the cavity voltage and the equivalent driving current from the generator should be in phase as follows:

$$\phi=\theta \quad . \tag{30}$$

Substituting this into Eq. (29) to obtain $\arg\left(\overrightarrow{v_{e,2}}\right)-\arg\left(\overrightarrow{v_{e,1}}\right)=-\psi$, and using Eq. (26), $\overrightarrow{v_{e,1}}$ can be expressed as follows:

$$\overrightarrow{v_{e,1}}=v_{e,1}e^{i\psi} \quad . \tag{31}$$

Similarly, the phase difference at steady state II between $\overrightarrow{v_{b,2}}$ and $\overrightarrow{v_{g,2}}$ is equal to that between $\overrightarrow{V_{b,2}}$ and $\overrightarrow{V_{g,2}}$:

$$\arg\left(\overrightarrow{v_{b,2}}\right)-\arg\left(\overrightarrow{v_{g,2}}\right)=\arg\left(\overrightarrow{V_{b,2}}\right)-\arg\left(\overrightarrow{V_{g,2}}\right). \tag{32}$$

At steady state II, the phases of the generator-induced voltage $\overrightarrow{V_{g,2}}$ and beam-induced voltage $\overrightarrow{V_{b,2}}$ are $\arg\left(\overrightarrow{V_{g,2}}\right)=\theta+\psi$ and $\arg\left(\overrightarrow{V_{b,2}}\right)=\pi+\psi$, respectively. Substituting them into Eq. (32) results in the following:

$$\arg\left(\overrightarrow{v_{b,2}}\right)-\arg\left(\overrightarrow{v_{g,2}}\right)=\pi-\theta \quad . \tag{33}$$

At steady state I, the radiated wave $\overrightarrow{v_{e,1}}$ is entirely depends on the generator because the cavity voltage $\overrightarrow{V_{c,1}}$ is induced by the generator alone:

$$\overrightarrow{v_{e,1}}=\overrightarrow{v_{g,1}} \quad . \tag{34}$$

Note that the forward power from the generator remains constant during stages I and II; therefore, the following can be obtained:

$$\overrightarrow{v_{g,2}}=\overrightarrow{v_{g,1}} \quad . \tag{35}$$

The following can be obtained by using the two expressions above and Eq. (31):

$$\overrightarrow{v_{g,2}}=v_{e,1}e^{i\psi} \quad . \tag{36}$$

The expressions above, Eq. (22), and Eq. (33) can be used to obtain the following:

$$\overrightarrow{v_{b,2}}=v_{f,2}e^{i(\pi-\theta+\psi)} \quad . \tag{37}$$

Using Eq. (12), $\overrightarrow{v_{b,2}}$ can be rewritten as follows:

$$\overrightarrow{v_{b,2}}=\sqrt{P_{g,2}}e^{i(\pi-\theta+\psi)} \quad . \tag{38}$$

Using the above expression with Eqs. (25), (26), and (35), the phasor relationship diagram of the various voltage waves in the waveguide can be obtained as shown in Fig. 2.

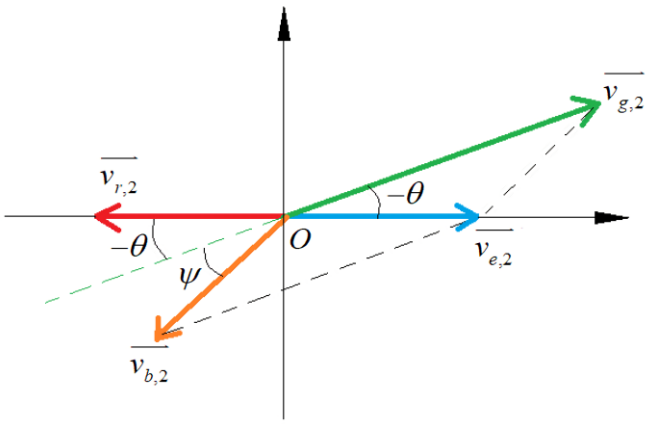

Fig. 2 Phasor relationship diagram of the voltage waves in the waveguide

Substituting Eqs. (26), (35) and (37) into Eq. (16) with the phase relationships at steady state II in Eqs. (5) and (30) to solve the resultant equation obtains $v_{e,1} = 2v_{f,2}\cos\psi$, which is then substituted into Eq. (36) to obtain the following equation:

$$\overrightarrow{v_{g,2}} = 2v_{f,2}\cos\psi e^{i\psi} \quad . \tag{39}$$

Using Eq. (12), the expression above can be rewritten as follows:

$$\overrightarrow{v_{g,2}} = 2\sqrt{P_{g,2}}\cos\psi e^{i\psi} \quad . \tag{40}$$

4 Modeling the RF behavior of the fundamental power coupler

4.1 Reflected wave and generator-induced radiated wave

Generalization of Eqs. (25) and (40), assuming that they are always true for a fundamental power coupler in the case of extreme over-coupling, can be expressed as follows:

$$\overrightarrow{v_r} \equiv -v_f \quad , \tag{41}$$

$$\text{and} \quad \overrightarrow{v_g} = 2\sqrt{P_g}\cos\psi e^{i\psi} \quad . \tag{42}$$

Eq. (41) indicates that the forward wave from the generator is always completely reflected by the coupler. Using Eq. (12), Eq. (41) can be rewritten as follows:

$$\overrightarrow{v_r} = -\sqrt{P_g} \quad . \tag{43}$$

4.2 Beam-induced radiated wave

To calculate the transient backward power in the waveguide, it is necessary to generalize Eq.(38). To simplify the problem, the case where the field in the cavity is induced solely by the beam was analyzed to obtain the general expression for the beam-induced radiated wave, because the field in the cavity satisfies the principle of linear superposition.

When the field in the cavity is induced solely by the beam, the power radiating from the cavity through the coupler can be obtained using Eqs. (16) and (11) as follows:

$$P_e = v_e^2 = v_b^2 \quad . \tag{44}$$

Meanwhile, the corresponding coupling factor β can be expressed as follows:

$$\beta = \frac{P_e}{P_{c,b}} = \frac{r_c v_b^{\,2}}{V_b^{\,2}} \propto \frac{v_b^{\,2}}{V_b^{\,2}} \quad , \tag{45}$$

where $P_{c,b} = V_b^{\,2}/r_c$ is the power loss in the cavity wall owing to the beam-induced field in the cavity.

With Eq. (45), the following is obtained:

$$v_b \propto \sqrt{\beta} V_b \quad . \tag{46}$$

According to the definition of the detuning angle, the beam-induced voltage V_b should conform to the following:

$$V_b \propto \cos\psi \, . \tag{47}$$

To deduce the relationship between V_b and β, a transient beam-loading process is simulated with Eqs. (1) - (4) for different values of β. At $t_0 = 0$, the CW beam injection begins and the field in the cavity is solely induced by the beam. The field in the cavity reaches a steady state after a sufficiently prolonged time and the detuning angle of the cavity remains constant throughout the entire process. The simulation result of the time evolution of the amplitude of the beam-induced voltage in this process is shown in Fig. 3, where V_b is the amplitude of the steady state beam-induced voltage corresponding to the coupling factor β_0.

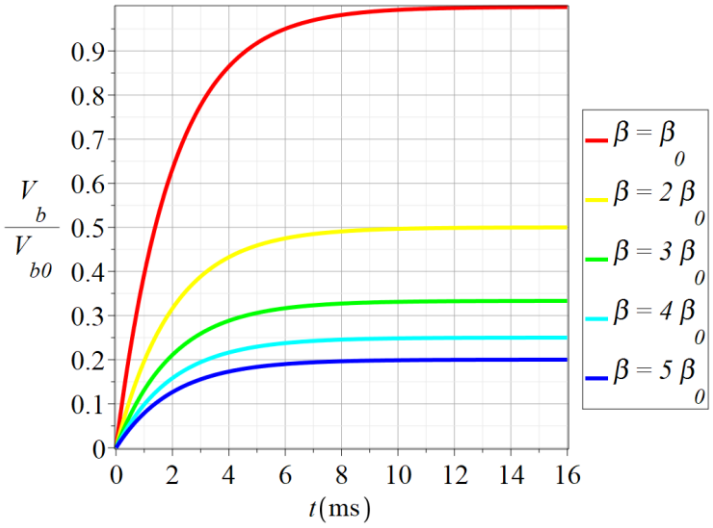

Fig. 3 (Color online) Time evolution of the amplitude of the beam-induced voltage

Based on Fig. 3, the steady-state value of V_b conforms to $V_b \propto \beta^{-1}$. Using Eqs. (46) and (47) the following is obtained:

$$v_b \propto \frac{\cos\psi}{\sqrt{\beta}} \quad . \tag{48}$$

Note that $v_{b,2}$ is for the optimum detuning and coupling; therefore, the general expression for v_b is as follows:

$$v_{\mathrm{b}}=\frac{\cos\psi}{\cos\psi_{\mathrm{opt}}}\sqrt{\frac{\beta_{\mathrm{opt}}}{\beta}}v_{\mathrm{b},2}\quad . \tag{49}$$

By assuming that the phase shift of the wave transmitted through the coupler remains constant irrespective of the coupling factor β, i.e., $\overrightarrow{v_{\mathrm{b}}}\parallel\overrightarrow{v_{\mathrm{b},2}}$, and noting that $\cos\psi$ and $\cos\psi_{\mathrm{opt}}$ are both real, β and β_{opt} are both real and positive, the following can be derived from the above relationship:

$$\overrightarrow{v_{\mathrm{b}}}=\frac{\cos\psi}{\cos\psi_{\mathrm{opt}}}\sqrt{\frac{\beta_{\mathrm{opt}}}{\beta}}\overrightarrow{v_{\mathrm{b},2}}\,. \tag{50}$$

Substituting Eq. (38) into the above expression results in the following:

$$\overrightarrow{v_{\mathrm{b}}}=\frac{\cos\psi}{\cos\psi_{\mathrm{opt}}}\sqrt{\frac{\beta_{\mathrm{opt}}P_{\mathrm{g},2}}{\beta}}e^{i(\pi-\theta+\psi)}\quad . \tag{51}$$

Using the following relationships in an extreme over-coupling superconducting cavity [14],

$$\begin{cases}\psi_{\mathrm{opt}}\approx-\phi\\ \beta_{\mathrm{opt}}\approx\dfrac{P_{\mathrm{b}}}{P_{\mathrm{c}}}=\dfrac{r_{\mathrm{c}}P_{\mathrm{b}}}{V_{\mathrm{c}}^{2}}\\ P_{\mathrm{g},2}\approx P_{\mathrm{b}}=I_{\mathrm{b0}}T_{\mathrm{tf}}e^{-\frac{\Delta\phi_{\mathrm{b}}^{2}}{2}}V_{\mathrm{c}}\cos\phi\\ \dfrac{r_{\mathrm{c}}}{\beta}\approx r_{\mathrm{L}}=\left(\dfrac{r}{Q}\right)Q_{\mathrm{L}}\end{cases}\quad . \tag{52}$$

Eq. (51) can be converted to the following:

$$\overrightarrow{v_{\mathrm{b}}}=I_{\mathrm{b0}}T_{\mathrm{tf}}e^{-\frac{\Delta\phi_{\mathrm{b}}^{2}}{2}}\sqrt{\left(\frac{r}{Q}\right)Q_{\mathrm{L}}}\cos\psi e^{i(\pi-\theta+\psi)}\quad . \tag{53}$$

4.3 Phenomenological model of the fundamental power coupler

Using Eqs. (42), (43), and (53), the steady-state phenomenological model of the fundamental power coupler for a superconducting cavity with the Gaussian bunched beam loading are formulated as follows:

$$\begin{cases}\overrightarrow{v_{\mathrm{r}}}=-\sqrt{P_{\mathrm{g}}}\\ \overrightarrow{v_{\mathrm{g}}}=2\sqrt{P_{\mathrm{g}}}\cos\psi e^{\mathrm{i}\psi}\\ \overrightarrow{v_{\mathrm{b}}}=I_{\mathrm{b0}}T_{\mathrm{tf}}e^{-\frac{\Delta\phi_{\mathrm{b}}^{2}}{2}}\sqrt{\left(\dfrac{r}{Q}\right)Q_{\mathrm{L}}}\cos\psi e^{\mathrm{i}(\pi-\theta+\psi)}\end{cases}\quad . \tag{54}$$

By replacing the beamform factor $\exp\left(-\Delta\phi_{\mathrm{b}}^{2}/2\right)$ in Eq. (53) with the corresponding equation, the phenomenological model of the coupler for other statistical distributions of the beam bunch can be readily obtained. For cases where the beam consists of short bunches, the beam form factor can be simply approximated as 1. In a case without beam loading, substituting $I_{\mathrm{b0}}=0$ into Eq. (53) obtains $\overrightarrow{v_{\mathrm{b}}}=0$, and the phenomenological model of the coupler is further simplified.

Using Eqs. (13), (16), and (11), the backward wave is obtained as follows:

$$\overrightarrow{v_{\mathrm{bk}}} = \overrightarrow{v_{\mathrm{r}}} + \overrightarrow{v_{\mathrm{g}}} + \overrightarrow{v_{\mathrm{b}}} \quad , \tag{55}$$

and the corresponding backward power is as follows:

$$P_{\mathrm{r}} = {v_{\mathrm{bk}}}^2 = \overrightarrow{v_{\mathrm{bk}}} \cdot \overrightarrow{v_{\mathrm{bk}}}^* \quad , \tag{56}$$

where $\overrightarrow{v_{\mathrm{bk}}}^*$ denotes the conjugate of a complex quantity $\overrightarrow{v_{\mathrm{bk}}}$.

Note that Eqs. (3) and (4) requires $P_{\mathrm{g}}(t)$ and $I_{\mathrm{b0}}(t)$ keeping constant for a short duration which is much larger than the cavity time constant after each time of their variations .

If $P_{\mathrm{g}}(t)$ and $I_{\mathrm{b0}}(t)$ can be approximated to be constant during a short duration after each time of their variations, and while accounting for the cavity detuning $\Delta\omega$ and cavity filling process characterized by the cavity time constant τ , a complex detuning attenuation factor $\vec{A}(t)$ can be obtained as follows:

$$\vec{A}(t) = \exp\left[-\left(i\Delta\omega + \frac{1}{\tau}\right)t\right] \quad , \tag{57}$$

and its counterpart, a complex detuning growth factor $\vec{B}(t)$, can be derived as follows:

$$\vec{B}(t) = 1 - \vec{A}(t) = 1 - \exp\left[-\left(i\Delta\omega + \frac{1}{\tau}\right)t\right] \quad . \tag{58}$$

The transient-state phenomenological model of the fundamental power coupler can be obtained by multiplying the corresponding factor to each expression in Eq. (54), with which the transient power reflected from the superconducting cavity in various beam-loading processes can be easily calculated using algebraic operations.

Using the phenomenological model of the fundamental power coupler formulated by Eqs. (54) - (58), the calculation of the transient power reflected from a superconducting cavity is converted from the cavity-side of the generator-coupler-cavity system to the generator-side, thus eliminating the complexity involved in the time evolution of the cavity fields during the beam loading process. Therefore, this phenomenological model can significantly simplify the calculation.

5 Verification and application of the phenomenological model

5.1 Transient beam loading process A

To validate the phenomenological model of the coupler, the time evolution of the reflected power from the superconducting cavity during the transient beam-loading process from Section 2 was recalculated using the phenomenological model of the fundamental power coupler that was formulated using Eqs. (54) - (58). The following process exemplifies the procedure for calculating the transient reflected power from the cavity using this phenomenological model.

Stage I: At $t = 0$, the generator is powered up, and $P_{\mathrm{g}} = P_{\mathrm{g,1}}$; since the beam is absent, $I_{\mathrm{b0}} = 0$. Substituting these values into Eq. (54), $\overrightarrow{v_{\mathrm{r,1}}}$ and $\overrightarrow{v_{\mathrm{b,1}}}$ can be obtain as follows:

$$\overrightarrow{v_{\mathrm{r,1}}}(t) \equiv -\sqrt{P_{\mathrm{g,1}}} \quad , \tag{59}$$

$$\text{and} \quad \overrightarrow{v_{\mathrm{b},1}}(t) \equiv 0 \quad . \tag{60}$$

The corresponding steady-state generator-induced radiated-wave $\overrightarrow{v_{\mathrm{g}0,1}}$ can also be obtained using Eq. (54). By multiplying it with the growth factor, Eq. (58), the transient generator-induced radiated wave $\overrightarrow{v_{\mathrm{g},1}}(t)$ can be obtained as follows:

$$\overrightarrow{v_{\mathrm{g},1}}(t) = \overrightarrow{v_{\mathrm{g}0,1}} \cdot \vec{B}(t) = \overrightarrow{v_{\mathrm{g}0,1}} \cdot \left\{ 1 - \exp\left[-\left(i\Delta\omega + \frac{1}{\tau} \right) t \right] \right\} \quad . \tag{61}$$

Stage II: At $t = \Delta T$, the forward power from the generator remains constant, that is, $P_{\mathrm{g}} = P_{\mathrm{g},2} = P_{\mathrm{g},1}$; therefore, the following is obtained:

$$\overrightarrow{v_{\mathrm{r},2}}(t) = \overrightarrow{v_{\mathrm{r},1}}(t) = -\sqrt{P_{\mathrm{g},1}} \quad , \tag{62}$$

and

$$\overrightarrow{v_{\mathrm{g},2}}(t) = \overrightarrow{v_{\mathrm{g},1}}(t) \quad . \tag{63}$$

Beam injection begins with $I_{b0} = I_{b0,2}$; by substituting this into Eq. (54), the corresponding steady-state beam-induced radiated wave $\overrightarrow{v_{\mathrm{b}0,2}}$ can be obtained. Multiplying this by the growth factor obtained by Eq. (58) with the time displacement of ΔT, the transient beam-induced radiated wave $\overrightarrow{v_{\mathrm{b},2}}(t)$ can be obtained as follows:

$$\overrightarrow{v_{\mathrm{b},2}}(t) = \overrightarrow{v_{\mathrm{b}0,2}} \cdot \vec{B}(t \to t - \Delta T) = \overrightarrow{v_{\mathrm{b}}} \cdot \left\{ 1 - \exp\left[-\left(i\Delta\omega + \frac{1}{\tau} \right)(t - \Delta T) \right] \right\} \quad . \tag{64}$$

Stage III: At $t = 2\Delta T$, the generator is powered down, $P_{\mathrm{g}} = 0$, and is substituted into Eq. (54) to obtain the following:

$$\overrightarrow{v_{\mathrm{r},3}} = 0 \quad . \tag{65}$$

Multiplying $\overrightarrow{v_{\mathrm{g},2}}(t)$ in Eq. (63) using the attenuation factor in Eq. (57) with the time displacement of $2\Delta T$, the transient generator-induced radiated wave $\overrightarrow{v_{\mathrm{g},3}}(t)$ is obtained as follows:

$$\overrightarrow{v_{\mathrm{g},3}}(t) = \overrightarrow{v_{\mathrm{g},2}}(t) \cdot \vec{A}(t \to t - 2\Delta T) = \overrightarrow{v_{\mathrm{g},2}}(t) \cdot \exp\left[-\left(i\Delta\omega + \frac{1}{\tau} \right)(t - 2\Delta T) \right] \quad . \tag{66}$$

Because the beam current intensity remains constant, the following can be obtained:

$$\overrightarrow{v_{\mathrm{b},3}}(t) = \overrightarrow{v_{\mathrm{b},2}}(t) \quad . \tag{67}$$

Stage IV: At $t = 3\Delta T$, the generator is powered up again, and $P_{\mathrm{g}} = P_{\mathrm{g},4}$. Substituting into Eq. (54) results in the following:

$$\overrightarrow{v_{\mathrm{r},4}} = -\sqrt{P_{\mathrm{g},4}} \quad . \tag{68}$$

Using Eq. (54), the corresponding steady-state generator-induced radiated wave $\overrightarrow{v_{\mathrm{g}0,4}}$ can also be obtained. Multiplying this by the growth factor, Eq. (58), with the time displacement of

$3\Delta T$, the transient generator-induced radiated wave $\overrightarrow{v_{g,4}}(t)$ can be obtained (the contribution from $\overrightarrow{v_{g,3}}(t)$ at this stage is negligible because it is sufficiently attenuated).

$$\overrightarrow{v_{g,4}}(t)=\overrightarrow{v_{g0,4}}\cdot\vec{B}(t\to t-3\Delta T)=\overrightarrow{v_{g0,4}}\cdot\left\{1-\exp\left[-\left(i\Delta\omega+\frac{1}{\tau}\right)(t-3\Delta T)\right]\right\} \quad . \tag{69}$$

Because the beam current intensity remains constant, the following is obtained:

$$\overrightarrow{v_{b,4}}(t)=\overrightarrow{v_{b,3}}(t) \quad . \tag{70}$$

The transient reflected power in each stage of $P_{r,k}(t)$ ($k=1..4$) can be obtained by substituting the expression of each voltage wave in each stage of Eqs. (59) - Eq. (70) into Eq. (55) and further into Eq. (56). The time evolution of the reflected power from the cavity, $P_r(t)$, during the entire process can be obtained by splicing $P_{r,k}(t)$ according to the time sequence. By substituting the parameters listed in Table 1 into the resulting piecewise analytical expression for $P_r(t)$, the resulting time evolution of $P_r(t)$ is indicated by the yellow curve shown in Fig. 4. To verify this result, the time evolution of $P_r(t)$ obtained using Eqs. (1)–(4) is indicated by the red curves as a comparison. The thinner yellow curve is plotted above the thicker red curve; if the difference between the two results is sufficiently small, the yellow curve should be enclosed by the red curve, that is, the compound curve consisting of the red and yellow curves should have a closed red boundary. The red boundary of the compound curve is open only at one location where the sharp peak reaches its maximum; the relative difference between the two curves is only 1.91%.

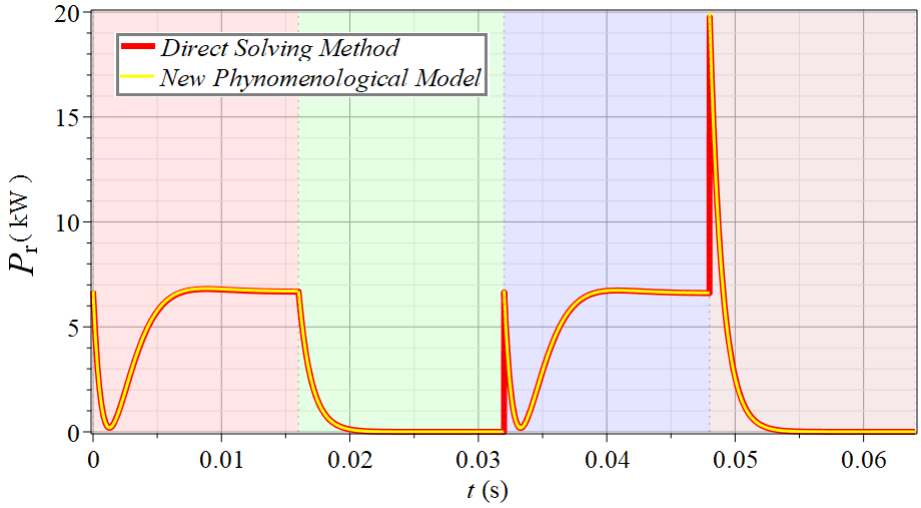

Fig. 4 Transient reflected power in process A

5.2 Transient beam loading process B

To further verify the phenomenological model, the reflected power was calculated in a more complex transient beam-loading process using Eqs. (54)–(58) under the time evolution of the generator power and beam current intensity, which is shown in Fig. 5. The calculation verifies where the cavity largely detunes causing a complicated trace of the cavity voltage on the complex plane. However, under real-world conditions, the likelihood of such a transient beam-loading process occurring is a low. In contrast to the previous transient beam loading process A, the time evolution of the generator power and beam current in this process varied between two nonzero values.

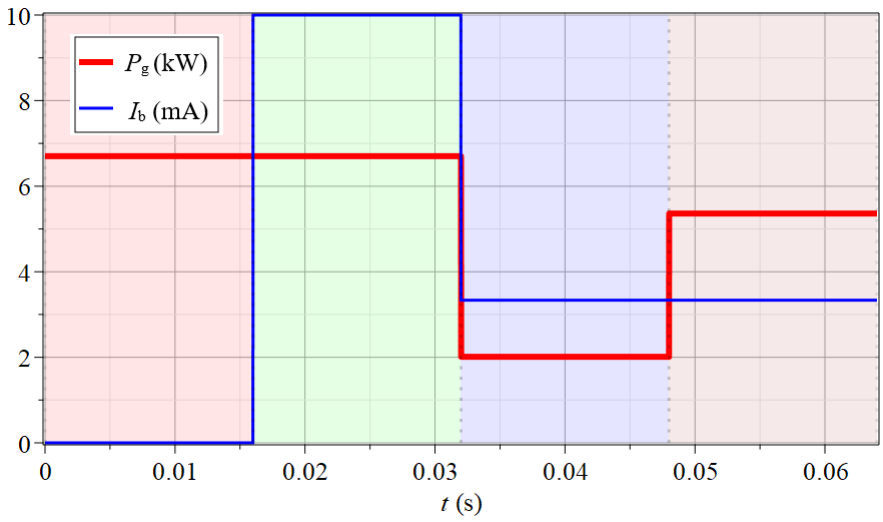

Fig. 5 Time evolution of the generator power and beam current in process B

The following calculation consists of two situations depending on the conditions of the cavity detuning and coupling.

Cavity Condition I

The cavity significantly deviates from its optimum detuning and coupling for the designed beam current in stage II, presenting a cavity detuning angle $\psi = 2\psi_{opt} = \pi/3$ and cavity coupling factor $\beta = \sqrt{2/3}\beta_{opt} \approx 653$ during the entire beam loading process. At $t_0 = 0$, the generator is powered up at 6.7 kW and the cavity field buildup process begins. At $t_1 = \Delta T$, the CW proton beam at the designed current of 10 mA is injected as the field in the cavity reaches a certain steady state I with an amplitude of 1.10 MV and phase 30.6º. Owing to the beam loading effects, the field in the cavity evolves to the steady state II with an amplitude of 0.61 MV and phase of -5.28º. At $t_2 = 2\Delta T$, the generator power suddenly shuts down and the beam continues to pass through the cavity at a current of 3.33 mA, which is 1/3 of the designed beam current, resulting in steady state III of the cavity field with an amplitude of 0.417 MV and phase of 13.4º. At $t_3 = 3\Delta T$, the generator power is partially recovered to 5.36 kW, and the field in the cavity evolves to the final steady state IV with an amplitude of 0.790 MV and phase of 21.6º. The corresponding trace of the cavity voltage on the complex plane during the entire beam loading process is shown in Fig. 6 (a); the trace form is significantly different than that shown in Fig. 1 (b), where the cavity is under optimum detuning and coupling for the designed beam current at stage II.

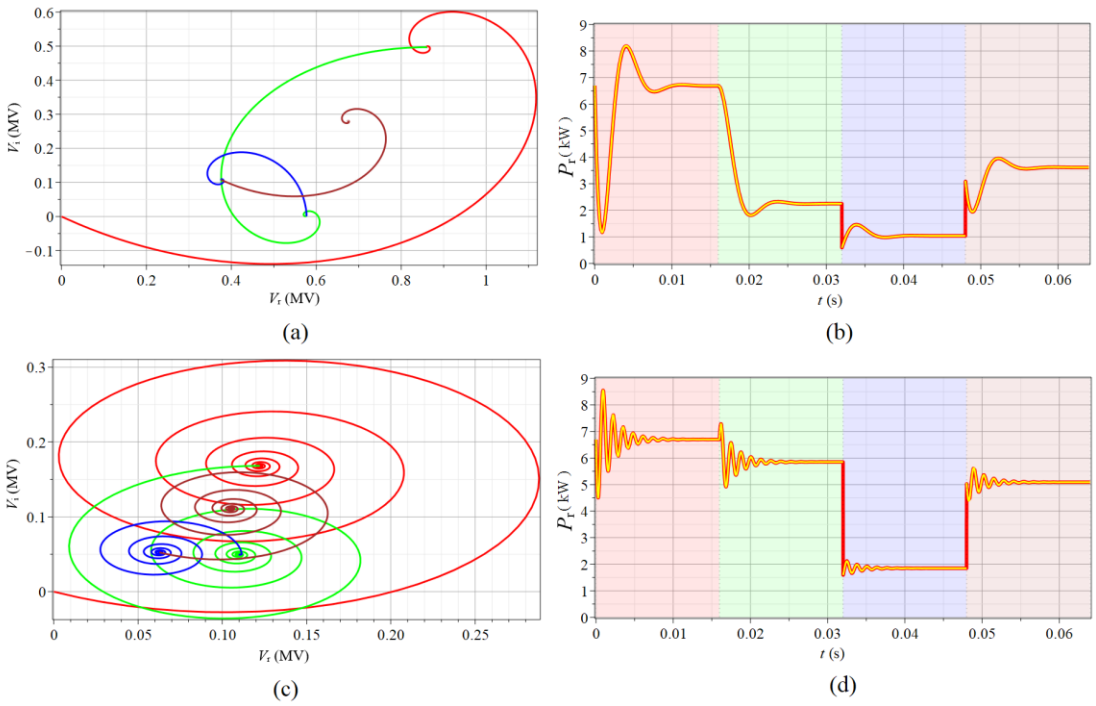

Fig. 6 (Color online) Trace of the cavity voltage and transient reflected power:
(a) and (b) demonstrate moderate detuning, whereas (c) and (d) demonstrate extreme detuning.

For brevity, only the expression for $\overrightarrow{v_{g,3}}$ in phase III during this beam-loading process is given below as a demonstration. Stage III starts at $t = 2\Delta T$ and $\overrightarrow{v_{g,3}}(t)$, during which it can be viewed as a linear superposition of the following two sources:

1) $\overrightarrow{v_{g,2}}(t)$ induced by $P_{g,2}$ and all the previous sources $P_{g,i}$ for $t < 2\Delta T$.

2) $\overrightarrow{v_{g,3}}'(t)$ induced by the new source $P_{g,3}$ for $t \geq 2\Delta T$.

At $t = 2\Delta T$, $P_{g,2}$ jumps to $P_{g,3}$, the sources of $\overrightarrow{v_{g,2}}(t)$ vanish, and $\overrightarrow{v_{g,2}}(t)$ in stage III is attenuated.

$$\overrightarrow{v_{g,2}}(t) = \overrightarrow{v_{g,2}}(2\Delta T) \cdot \vec{A}(t \to t - 2\Delta T). \tag{71}$$

Meanwhile, $\overrightarrow{v_{g,3}}'(t)$ starts to rise with its driving sources $P_{g,3}$:

$$\overrightarrow{v_{g,3}}'(t) = \overrightarrow{v_{g0,3}}' \cdot \vec{B}(t \to t - 2\Delta T), \tag{72}$$

where $\overrightarrow{v_{g0,3}}'$ corresponds to the steady-state value of $\overrightarrow{v_{g,3}}'$ determined using Eq. (54).

Using the above two expressions, $\overrightarrow{v_{g,3}}(t)$ can be obtained as follows:

$$\begin{aligned} \overrightarrow{v_{g,3}}(t) &= \overrightarrow{v_{g,2}}(t) + \overrightarrow{v_{g,3}}'(t) \\ &= \overrightarrow{v_{g,2}}(2\Delta T) \cdot \vec{A}(t \to t - 2\Delta T) + \overrightarrow{v_{g0,3}}' \cdot \vec{B}(t \to t - 2\Delta T) \end{aligned}. \tag{73}$$

The expression for $\overrightarrow{v_{b,3}}(t)$ can be obtained in a similar manner.

By substituting the parameters listed in Table 1 to evaluate $P_r(t)$, the resulting curve is shown in yellow in Fig. 6 (b), whereas the red curve is obtained by directly solving Eqs. (1) - (4). The figure demonstrates that the red boundary of the compound curve is closed during the entire beam-loading process, implying that the transient reflected powers from the cavity obtained by the two

methods show sufficient agreement.

Cavity Condition II

The cavity is at extreme detuning with the detuning angle ψ = 7π/15, which approaches π/2 and significantly deviates from the optimum coupling for the designed beam current at stage II with the cavity coupling factor $\beta = \sqrt{2/3}\beta_{\mathrm{opt}} \approx 653$ during the entire beam-loading process. Owing to the extreme detuning of the cavity, the corresponding trace of the cavity voltage on the complex plane in this process becomes significantly more complicated than that in all the previous situations, as shown in Fig. 6 (c). By substituting the parameters listed in Table 1 to evaluate $P_{\mathrm{r}}(t)$, the resulting curve is shown in yellow in Fig. 6 (d), whereas the red curve is obtained via the direct solution of Eqs. (1) - (4). The red boundary of the compound curve is closed during the entire process, indicating that the transient reflected power from the cavity obtained by the two methods is in sufficient agreement, despite extreme cavity detuning. Note that the commonly used conventional method for numerically solving Eqs. (1) and (2) would be significantly time-consuming when dealing with the beam-loading process with a cavity detuning angle that is approaching π/2, as in this case.

Additional comparisons for various beam-loading processes and cavity conditions were conducted between the transient reflected power obtained from the phenomenological model using the formulated Eqs. (54)–(58) and that obtained by numerically solving Eqs. (1) and (2); the results were in sufficient conformance with each other as long as the cavity was extremely over-coupled.

5.3 Maximum reflected power during the cavity failure recovery process

As shown in Fig. 2, the peak of the transient reflected power occurs when the generator power is recovered while the beam continues to pass through the cavity during the period without the RF power feed from the generator, which is a realistic situation that occurs in an accelerator requiring an ultra-high beam availability, such as that in the CAFe Linac. The generator power driving the superconducting cavity is instantly cut off by the machine protection system to protect the cavity when the cavity quenches; thus, the trend of quenching is presented, or the instability of the cavity fields is detected. The generator power is restored after the problem of the cavity is resolved while the beam continues to pass through the cavity during the entire process. A technique for cavity failure recovery is currently under development for the CAFe Linac to ensure that its beam availability can eventually meet the ultrahigh demand of beam availability for the ADS application. Therefore, for such accelerators, it is critical to calculate the maximum reflected power during a cavity failure recovery process to provide indispensable information for the design of relevant parts of an RF system. By applying the phenomenological model formulated by Eqs. (54)–(58), this maximum value can be deduced without the specific parameters of the accelerator.

At the moment when the generator power is recovered, $\overrightarrow{V_{\mathrm{g}}} = 0$, and based on Eq. (17), $\overrightarrow{v_{\mathrm{g}}} = 0$; therefore, the backward wave can be expressed using Eqs. (54) and (55) as follows:

$$\begin{aligned}\overrightarrow{v_{\mathrm{bk}}} &= \vec{v_{\mathrm{r}}} + \vec{v_{\mathrm{b}}} = -\sqrt{P_{\mathrm{g}}} + I_{\mathrm{b0}} T_{\mathrm{tf}} e^{-\frac{\Delta\phi_b^2}{2}} \sqrt{\left(\frac{r}{Q}\right) Q_{\mathrm{L}}} \cos\psi e^{\mathrm{i}(\pi-\theta+\psi)} \\ &= -\sqrt{P_{\mathrm{g}}} + v_{\mathrm{b}} e^{\mathrm{i}(\pi-\theta+\psi)}\end{aligned} \quad , \tag{74}$$

and the amplitude of $\overrightarrow{v_{\mathrm{bk}}}$ is as follows:

$$v_{\mathrm{bk}} = \left|-\sqrt{P_{\mathrm{g}}} + v_{\mathrm{b}} e^{\mathrm{i}(\pi-\theta+\psi)}\right| \le \left|\sqrt{P_{\mathrm{g}}}\right| + \left|v_{\mathrm{b}}\right| \quad . \tag{75}$$

The equality expressed in Eq. (75) is only true if $-\sqrt{P_{\mathrm{g}}}$ and $v_{\mathrm{b}} e^{\mathrm{i}(\pi-\theta+\psi)}$ are in phase, where

$$\pi - \theta + \psi = \pi \tag{76}$$

or

$$\psi = \theta \,. \tag{77}$$

For a superconducting cavity accelerating CW or long macro–pulse beam, the cavity is usually optimally detuned to minimize the required RF power from the generator, and using the first equation in Eq.(52), the following is obtained:

$$\psi = \psi_{\mathrm{opt}} = -\theta \quad . \tag{78}$$

Eqs. (77) and (78) result in the following:

$$\psi_{\mathrm{opt}} = \theta = 0 \quad , \tag{79}$$

which represents the on-crest acceleration of an ultra-relativistic beam.

Furthermore, the maximum amplitude of $\overrightarrow{v_{bk}}$ is as follows:

$$v_{\mathrm{bk,max}} = \left|\sqrt{P_{\mathrm{g}}}\right| + \left|v_{\mathrm{b}}\right| = \sqrt{P_{\mathrm{g}}} + v_{\mathrm{b}} \quad . \tag{80}$$

Using Eq. (22) to obtain $v_{\mathrm{b}} = v_{\mathrm{r}} = \sqrt{P_{\mathrm{g}}}$ under an optimum detuning and coupling with the designed beam current, $v_{bk,\mathrm{max}}$ can be further simplified to the following:

$$v_{bk,\mathrm{max}} = 2\sqrt{P_g} \quad , \tag{81}$$

and the corresponding maximum backward power, or the reflected power from the cavity, $P_{r,\mathrm{max}}$,is written as follows:

$$P_{\mathrm{r,max}} = v_{\mathrm{bk,max}}{}^2 = 4P_{\mathrm{g}} \quad . \tag{82}$$

This indicates that the upper limit of the transient reflected power during the cavity failure recovery process is four times that of the forward generator power for a superconducting cavity under optimum detuning and coupling to the acceleration of the beam at the designed current. Therefore, the design of the relevant parts of an RF system should incorporate a transient power surge five times (including a one-time contribution from the forward generator power) that of the forward generator power to ensure the safety of the instrument under such conditions.

6 Conclusion

Using the phenomenological model of the RF behavior of the fundamental power coupler

formulated using Eqs. (54)–(58), the mathematical calculations for the evaluation of the transient power reflected from a superconducting cavity in the presence of beam loading can eventually be converted to algebraic operations without solving the relevant differential equation numerically. This can be done while maintaining the calculation accuracy, which signifies the vast simplification of the conventional calculation process and significant reduction in the computational time, especially in the early design stage of parameter optimization. Moreover, for the beam-loading process, the difference between the theoretical results predicted by solving Eqs. (1)–(2) and the corresponding experimental values can typically reach 5%, which is larger than the difference in the results from the phenomenological model and directly solving the corresponding differential equation, indicating that the phenomenological model is sufficient to predict the transient reflected power in such a process.

Meanwhile, the simple and vivid physical demonstration provided by this phenomenological model can facilitate an intuitive understanding of the time evolution of the reflected power from the superconducting cavity in various transient beam-loading processes, especially the significant surge in the reflected power during a certain beam-loading process, such as that simulated in Sect. 2. To a certain extent, the phenomenological model can be regarded as an extension of the classical transmission line theory of microwave engineering, where a radiated wave emerging from an extremely over-coupled active microwave impedance is introduced under the circumstance of the superconducting acceleration.

Note that by using a simple beam-loading process to deduce the phenomenological model, the model may appear to be valid only for the beam-loading process with a simple time evolution of the generator power and beam-current intensity. However, the model can be validated for any transient beam-loading process because the time evolution of excitations described by an arbitrary continuous curve can always be approximately described by a staircase-like polygonal curve similar to Eq. (3), where a piecewise function with more nodes is required to approximate the original curve for the time evolution of a more complex excitation. For each stage of the piecewise function, the duration needn't to be significantly longer than the cavity time constant to reach the corresponding steady state, instead, it can be significantly shorter than the cavity time constant to describe a notably more rapid process.

The method reported in this study based on the phenomenological model of the RF behavior of the fundamental power coupler was successfully utilized in the transient RF analysis of the superconducting cavity system of the CAFe Linac over the past several years and has achieved satisfactory results, while vastly simplifying the calculation process and significantly reducing the computational time.

References

[1] Y. He, W. Yue, S. Zhang et al., SRF cavities for ADS project in China. Proc. 16th Int. Conf. RF Superconductivity. 868–872 (2013). Available at https://accelconf.web.cern.ch/srf2013/papers/thiod01.pdf

[2] H. Li, P. Sha, J. Dai et al., Design study on very low Beta spoke cavity for China-ADS. Chinese Phys. C 36, 761 (2012). doi 10.1088/1674-1137/36/8/014

[3] W. Yue, S. Zhang, C. Li et al., Development of a low beta half-wave superconducting cavity

and its improvement from mechanical point of view. Nucl. Instrum. Methods Phys. Res. A 953, 163259 (2020). https://doi.org/10.1016/j.nima.2019.163259
[4] W. Yue, S. Zhang, C. Li et al., Design, fabrication and test of a taper-type half-wave superconducting cavity with the optimal beta of 0.15 at IMP. Nucl. Eng. Technol. 52, 1777–1783 (2020). https://doi.org/10.1016/j.net.2020.01.014
[5] F. Yan, H. Geng, C. Meng et al., Commissioning experiences with the spoke-based CW superconducting proton linac. Nucl. Sci. Tech. 32, 105 (2021). https://doi.org/10.1007/s41365-021-00950-7
[6] X. Wan, X. Pu, Z. Ren et al., Discussion of 90° stopband in low-energy superconducting linear accelerators. Nucl. Sci. Tech. 33, 121(2022). https://doi.org/10.1007/s41365-022-01104-z
[7] A. S. Dhavale, K. C. Mittal, Evaluation of external Q of the superconducting cavity using Kroll-Yu method, Rev. Sci. Instrum. 77, 066101 (2006). https://doi.org/10.1063/1.2204921
[8] A. Wu, S. Zhang, W. Yue, et al., Design study on medium beta superconducting half-wave resonator at IMP. Nucl. Sci. Tech. 27, 80 (2016). https://doi.org/10.1007/s41365-016-0081-y
[9] X. Sun, F. Chen, X. Yang et al., Superconducting multipole wiggler with large magnetic gap for HEPS-TF. Nucl. Sci. Tech. 33, 16 (2022). https://doi.org/10.1007/s41365-022-01001-5
[10] X. Niu, F. Bai, X. Wang, et al. Cryogenic system design for HIAF iLinac. Nucl. Sci. Tech. 30, 178 (2019). https://doi.org/10.1007/s41365-019-0700-5
[11] A. Sukhanov, E. Harms, A. Hocker, et al. High power tests of dressed superconducting 1.3 GHz RF cavities. Proc IPAC. 949-951 (2011). Available at https://accelconf.web.cern.ch/PAC2011/papers/tup071.pdf
[12] Y. Cheng, H. Zheng, H. Liu et al., Design of machine protection system for CAFe facility. Radiat. Detect. Technol. 4, 448–455 (2020). https://doi.org/10.1007/s41605-020-00196-8
[13] T. P. Wangler. RF linear accelerators. 2nd completely rev. and enl. ed. Weinheim: Wiley-VCH (2008). doi:10.1002/9783527623426
[14] H. Padamsee, J. Knobloch, T. Hays, RF superconductivity for accelerators. 2nd ed. Weinheim: Wiley-VCH (2008). ISBN: 978-3-527-40842-9
[15] C. Xu, Z. Zhu, F. Qiu et al., Application of a modified iterative learning control algorithm for superconducting radio-frequency cavities. Nucl. Instrum. Methods Phys. Res. A 1026, 166237 (2022). https://doi.org/10.1016/j.nima.2021.166237
[16] F. Qiu, S. Michizono, T. Matsumoto et al., Combined disturbance-observer-based control and iterative learning control design for pulsed superconducting radio frequency cavities. Nucl. Sci. Tech. 32, 56 (2021). https://doi.org/10.1007/s41365-021-00894-y
[17] F. Qiu, Y. He, A. Wu et al., In situ mitigation strategies for field emission-induced cavity faults using low-level radiofrequency system. Nucl. Sci. Tech. 33, 140–154 (2022). https://doi.org/10.1007/s41365-022-01125-8
[18] Q. Chen, Z. Gao, Z. Zhu et al., Multi-frequency point supported LLRF front-end for CiADS wide-bandwidth application. Nucl. Sci. Tech. 31, 29 (2020). https://doi.org/10.1007/s41365-020-0733-9
[19] J. Ma, F. Qiu, L. Shi et al., Precise calibration of cavity forward and reflected signals using low-level radio-frequency system. Nucl. Sci. Tech. 33, 4 (2022). https://doi.org/10.1007/s41365-022-00985-4
[20] L. Yang, H. Cao, J. Zhao et al., Development of a wide-range and fast-response digitizing pulse signal acquisition and processing system for neutron flux monitoring on EAST. Nucl. Sci. Tech.

33(3), 35 (2022). https://doi.org/10.1007/s41365-022-01016-y
[21] Y. He, Z. Wang, Y. Liu et al., The conceptual design of injector II of ADS in China. Proc IPAC., 2613-2615 (2011). Available at https://accelconf.web.cern.ch/ipac2011/papers/weps053.pdf
[22] S. Liu, Z. Wang, W. Yue et al., Full period superconducting section physics design for injector II of China-ADS. Chinese Phys. C 38(11), 117006 (2011). doi 10.1088/1674-1137/38/11/117006
[23] Y. He, Z. Wang, Z. Qin, et al. Development of accelerator driven advanced nuclear energy (ADANES) and nuclear fuel recycle. Proc. IPAC., 4389-4393 (2019). Available at https://accelconf.web.cern.ch/ipac2019/papers/tuypls2.pdf
[24] L. Chen, S. Zhang, Y. Li et al., Room-temperature test system for 162.5 MHz high-power couplers. Nucl. Sci. Tech. 30, 7 (2019). https://doi.org/10.1007/s41365-018-0531-9
[25] R. Huang, Y. He, Z. Wang et al., Analytical solution to the transient beam loading effects of a superconducting cavity. Chinese Phys. C 41, 107001 (2017). https://doi.org/10.1088/1674-1137/41/10/107001
[26] W. Yue, Y. He, S. Zhang et al., R&D of IMP Superconducting HWR for China ADS. Proc LINAC., 600-602 (2012). Available at https://inspirehep.net/files/8c9461feb8e0a7b264398edde9ff3dd7
[27] P.R. Karmel, G.D. Colef, R.L. Camisa, Introduction to electromagnetic and microwave engineering. John Wiley & Sons (1998). ISBN: 978-0-471-17781-4
[28] D. M. Pozar, Microwave engineering. 4th ed. Hoboken, NJ: Wiley (2012). ISBN: 978-1-118-29813-8